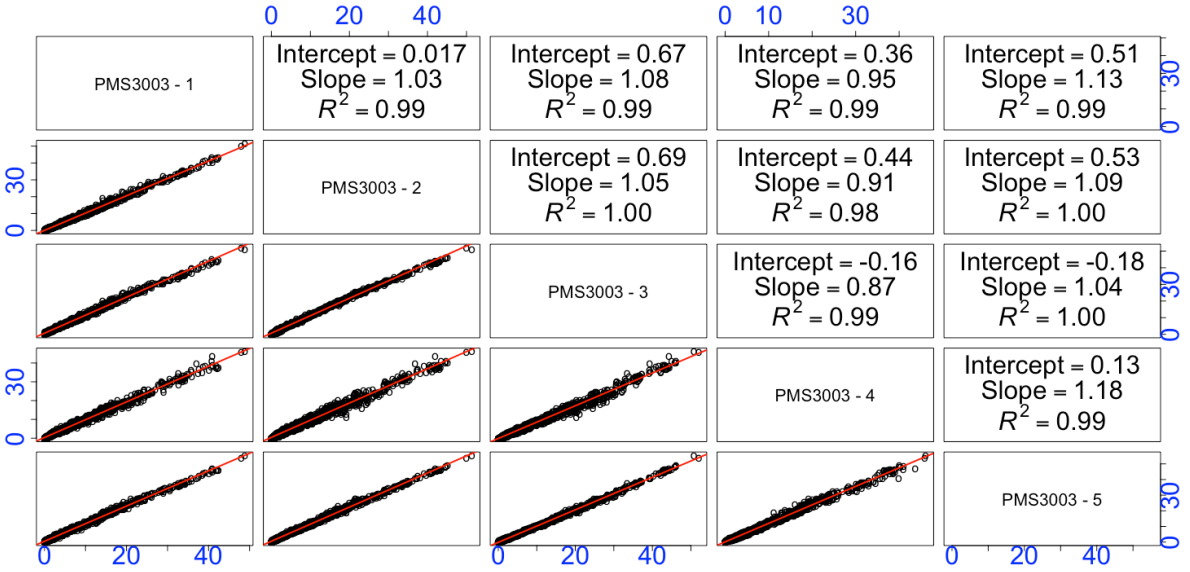

Figure S1: Pairwise correlations between 1 h aggregated $PM_{2.5}$ mass concentrations (µg m^{-3}) of the uncalibrated PMS3003s from February 1, 2017 to March 31, 2017 at Duke University. Upper-right set of panels: intercept, slope, and R^2 of linear regression models using the ordinary least squares (OLS) method. Lower-left set of panels: linear regression lines superimposed on pairwise plots.

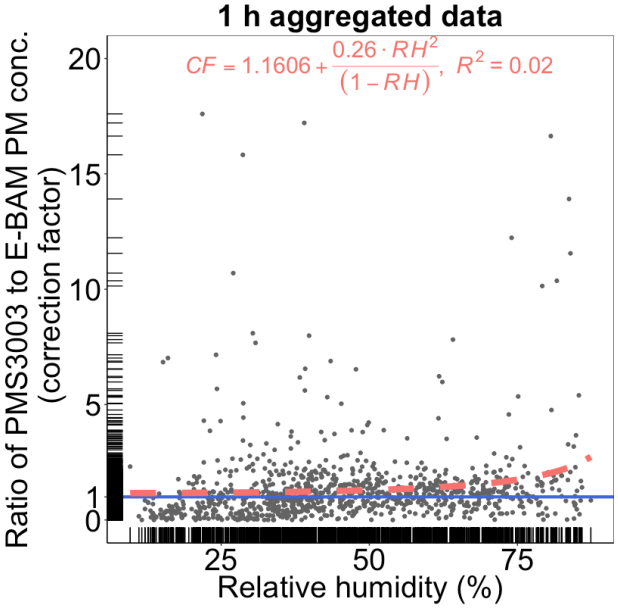

Figure S2: Fractional increase in $PM_{2.5}$ weight measured by uncalibrated PMS3003 sensors with respect to RH at 1 h time interval between February 1, 2017 and March 31, 2017 at Duke University (6 h, 12 h, and 24 h results not shown). RH (%) and PMS3003 $PM_{2.5}$ concentration (µg m^{-3}) data are arithmetic means averaged across all five PMS3003 sensor packages at each point in time. The fitted RH adjustment equation and curve were superimposed on the plot. Marginal rugs were added to better visualize the distribution of data on each axis. The blue line indicates ratio of 1.

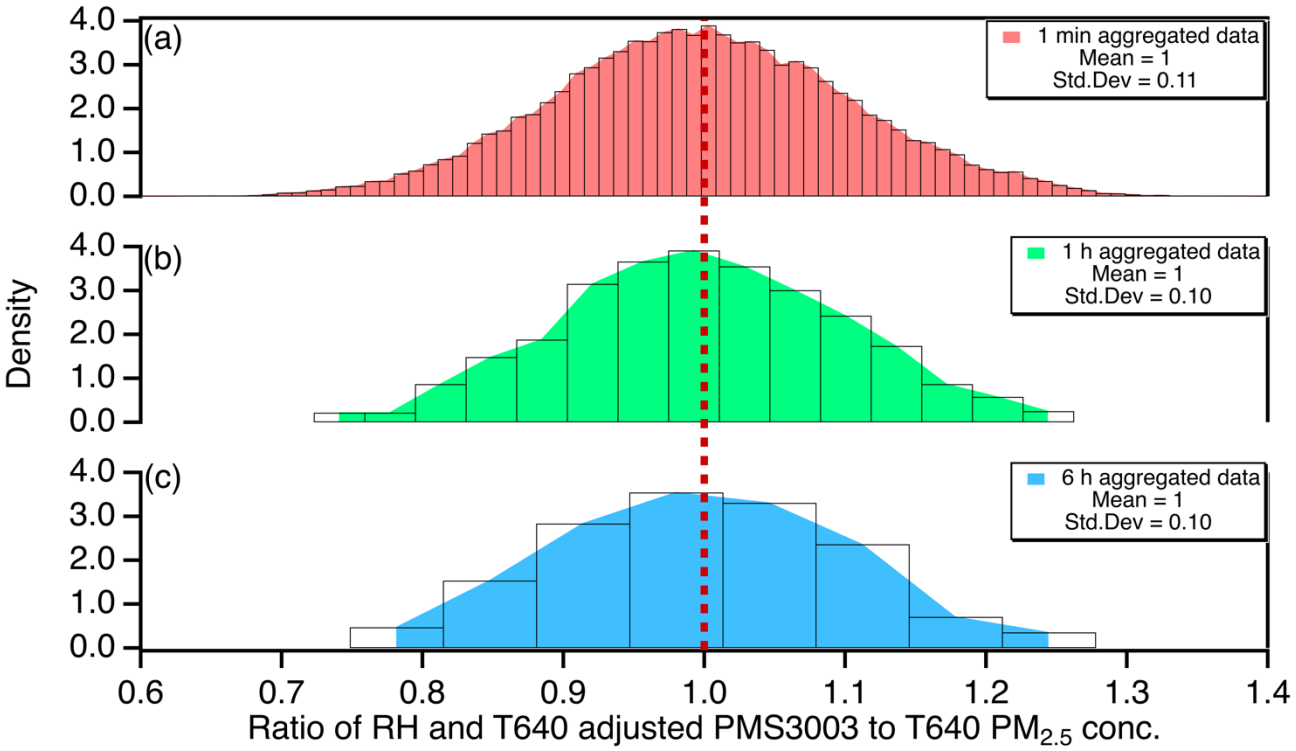

Figure S3: Histograms illustrating the distribution of the sets of ratios of RH and T640 adjusted PMS3003 to T640 $PM_{2.5}$ measurements at a) 1 min, b) 1 h, and c) 6 h time intervals from June 30, 2017 to July 31, 2017 at US EPA RTP. The ratios at each time interval are grouped in bins, and the optimal bin size at each time interval is calculated from Scott's equation (1979): $W = 3.49\ \sigma\ N^{-1/3}$ (where W is the bin width, σ is the Std.Dev of the distribution, and *N* is the number of observations). The height of each bar is expressed in density rather than frequency, and density is directly proportional to frequency. Superimposed on the histograms are the corresponding empirically estimated probability density functions (PDF). The red dashed line indicates the arithmetic mean of the set of ratios at each time interval. The mean and Std.Dev of each set of ratios are also displayed on the plots. Note only the statistically averaged sensor results at each time interval are shown.

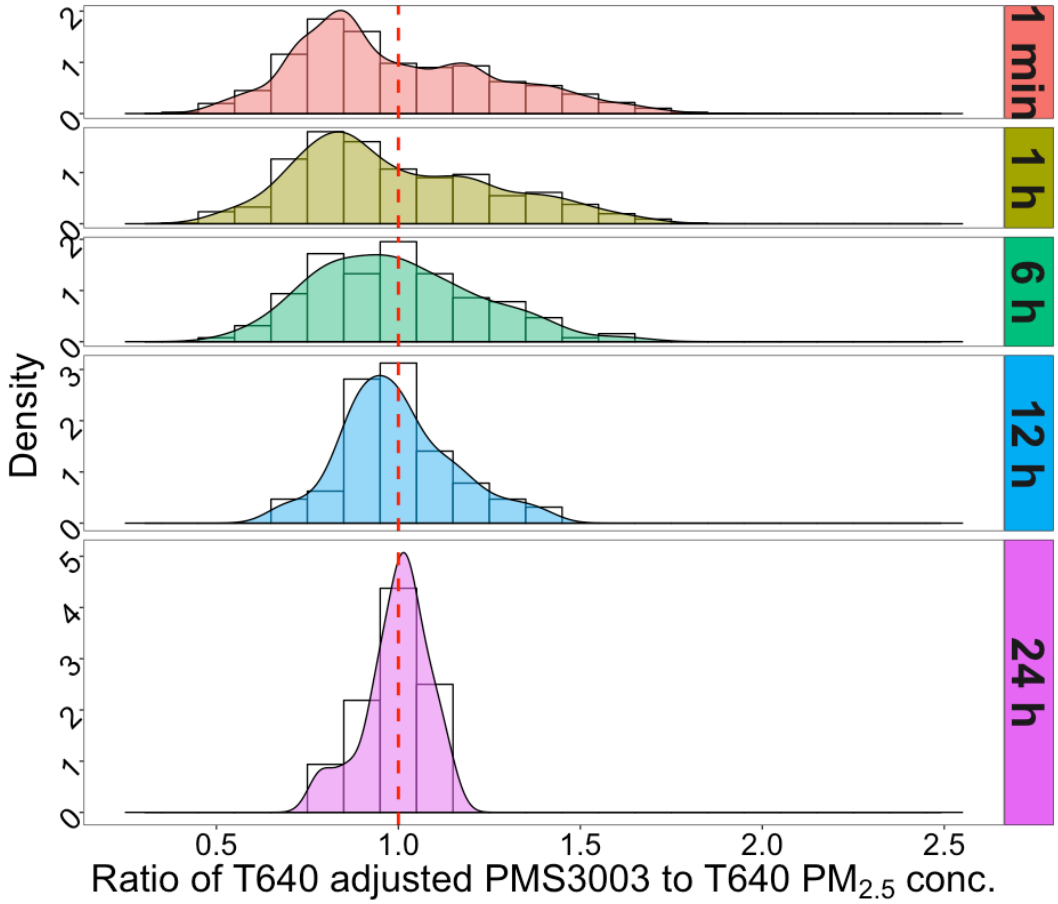

Figure S4: Histograms illustrating the distribution of the sets of ratios of T640 adjusted PMS3003 to T640 $PM_{2.5}$ measurements at 1 min, 1 h, 6 h, 12 h, and 24 h time intervals from June 30, 2017 to July 31, 2017 at US EPA RTP. The height of each bar is expressed in density rather than frequency, and density is directly proportional to frequency. Superimposed on the histograms are the corresponding empirically estimated probability density functions (PDF). The red dashed line indicates ratio of 1. Note only the statistically averaged sensor results at each time interval are shown.

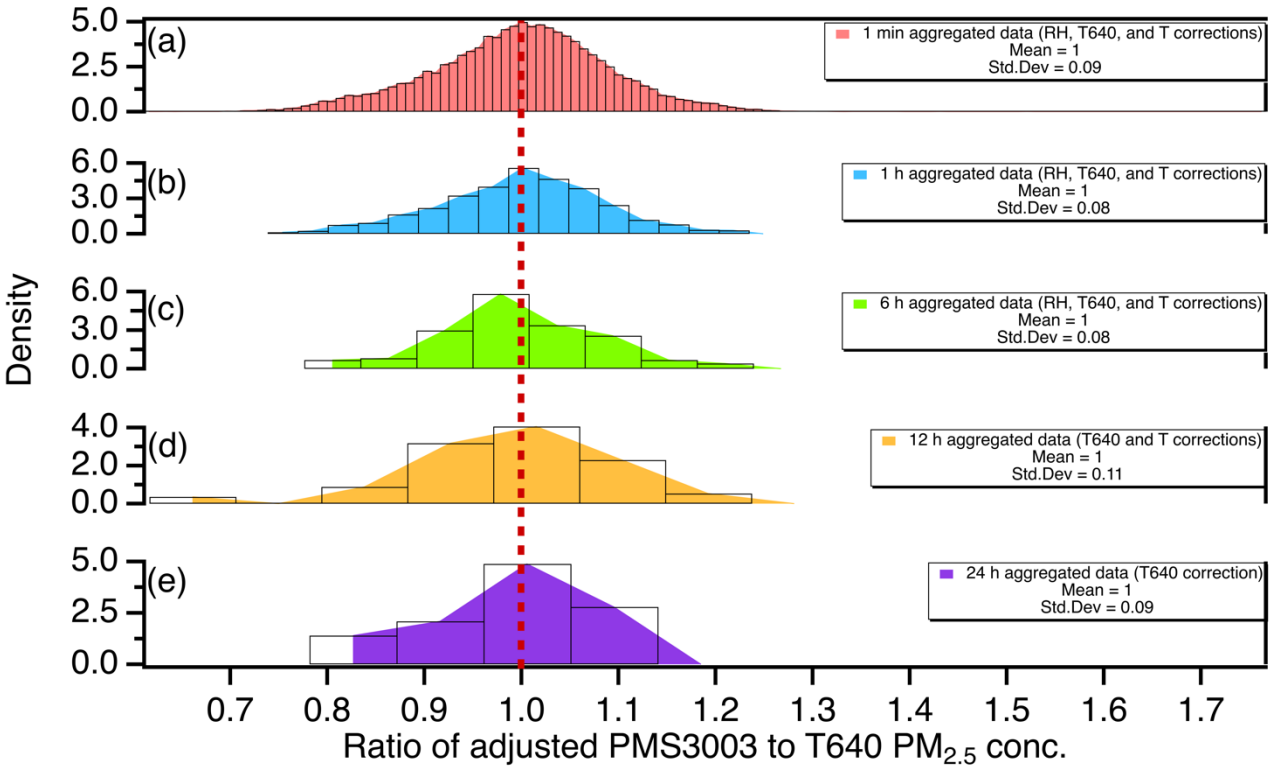

Figure S5: Histograms illustrating the distribution of the sets of ratios of calibrated PMS3003 to T640 $PM_{2.5}$ measurements at a) 1 min, b) 1 h, c) 6 h, d) 12 h, and e) 24 h time intervals from June 30, 2017 to July 31, 2017 at US EPA RTP. The temperature (T) correction is only valid for 1 min to 12 h aggregated data and the RH correction is only valid for 1 min to 6 h aggregated data. The ratios at each time interval are grouped in bins, and the optimal bin size at each time interval is calculated from Scott's equation (1979): $W = 3.49\ \sigma\ N^{-1/3}$ (where W is the bin width, σ is the Std.Dev of the distribution, and *N* is the number of observations). The height of each bar is expressed in density rather than frequency, and density is directly proportional to frequency. Superimposed on the histograms are the corresponding empirically estimated probability density functions (PDF). The red dashed line indicates the arithmetic mean of the set of ratios at each time interval. The mean and Std.Dev of each set of ratios are also displayed on the plots. Note only the statistically averaged sensor results at each time interval are shown.

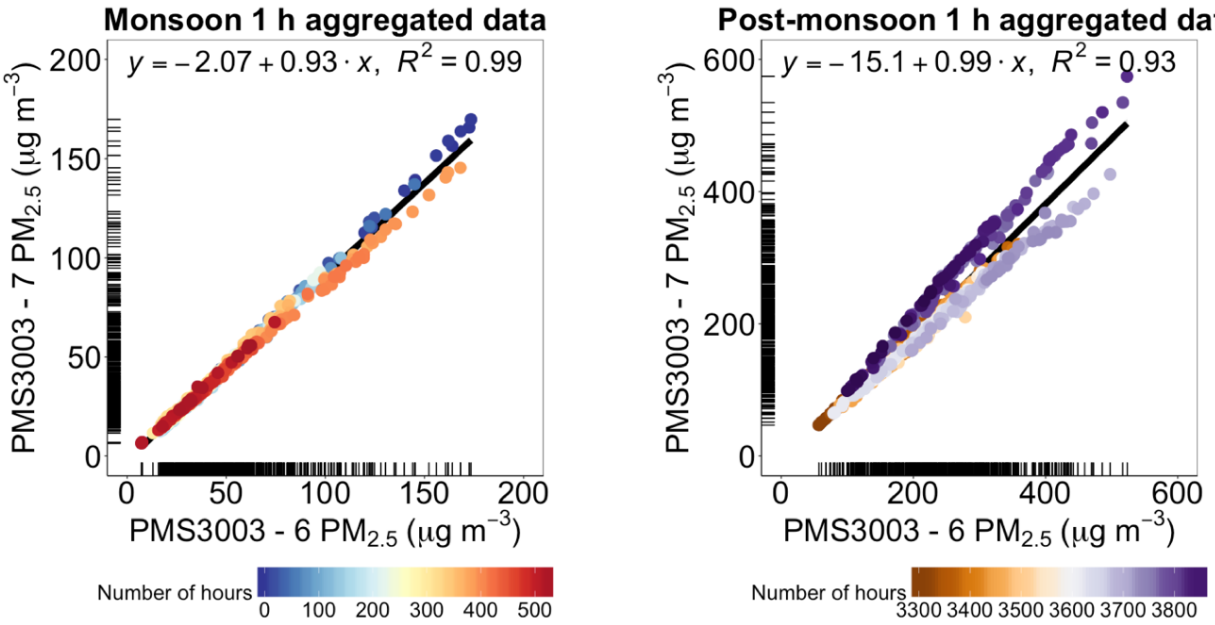

Figure S6: Linear regressions between aggregated $PM_{2.5}$ mass concentrations (µg m^{-3}) of the two uncalibrated PMS3003s at 1 h time interval during the monsoon season (from June 8, 2017 to June 29, 2017), and the post-monsoon season (from Oct 23, 2017 to Nov 16, 2017) at IIT Kanpur. Each data point was color coded by the number of hours past the beginning of the Kanpur study (i.e., 2017 June 08 00:00). Marginal rugs were added to better visualize the distribution of data on each axis.

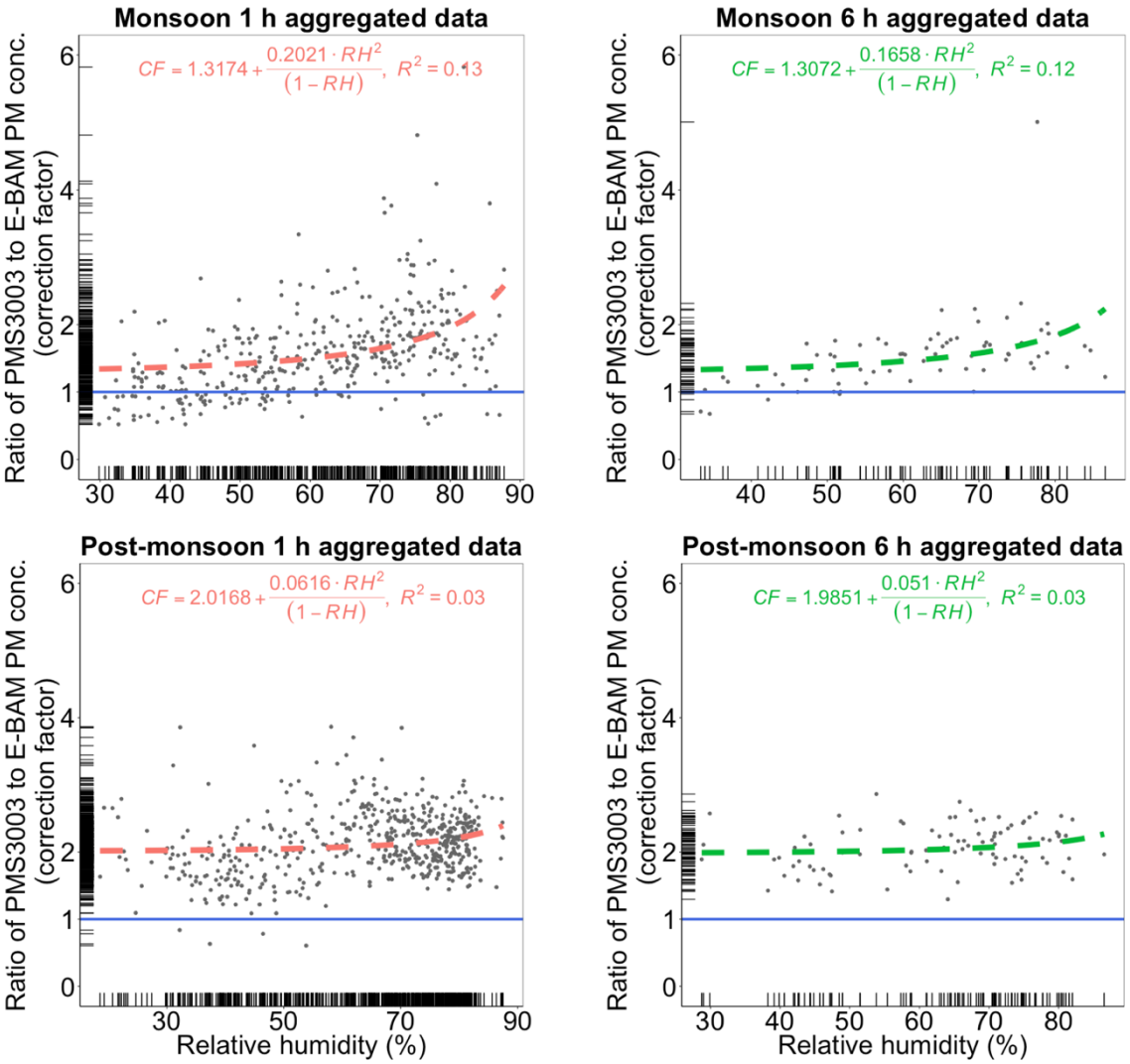

Figure S7: Fractional increase in $PM_{2.5}$ weight measured by uncalibrated PMS3003 sensors with respect to RH at 1 h and 6 h time intervals during the monsoon season (from June 8, 2017 to June 29, 2017), and the post-monsoon season (from Oct 23, 2017 to Nov 16, 2017) at IIT Kanpur. RH (%) and PMS3003 $PM_{2.5}$ concentrations (µg m^{-3}) are arithmetic means averaged across all the two PMS3003 sensor packages at each point in time. The fitted RH adjustment equations and curves were superimposed on the plots. Marginal rugs were added to better visualize the distribution of data on each axis. The blue lines indicate ratio of 1. The results of 12 h and 24 h aggregated data are not shown as their patterns are more indistinct than their 1 h and 6 h counterparts.

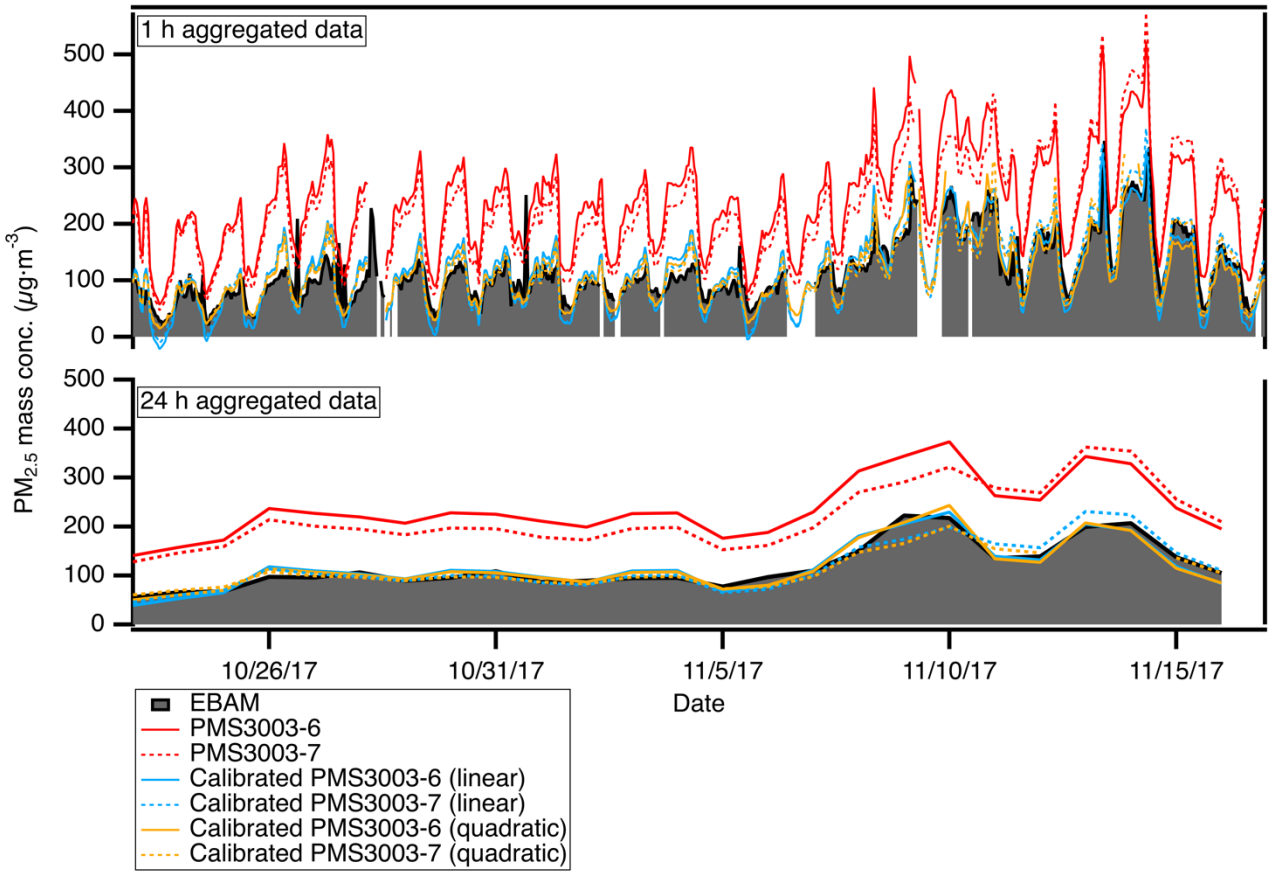

Figure S8: Comparison of 1 h and 24 h aggregated $PM_{2.5}$ mass concentrations between the E-BAM and the two PMS3003 sensor packages from Oct 23, 2017 to Nov 16, 2017 (post-monsoon season) at IIT Kanpur. Both the raw and calibrated sensor results (using simple linear regression and quadratic models) are shown.

5

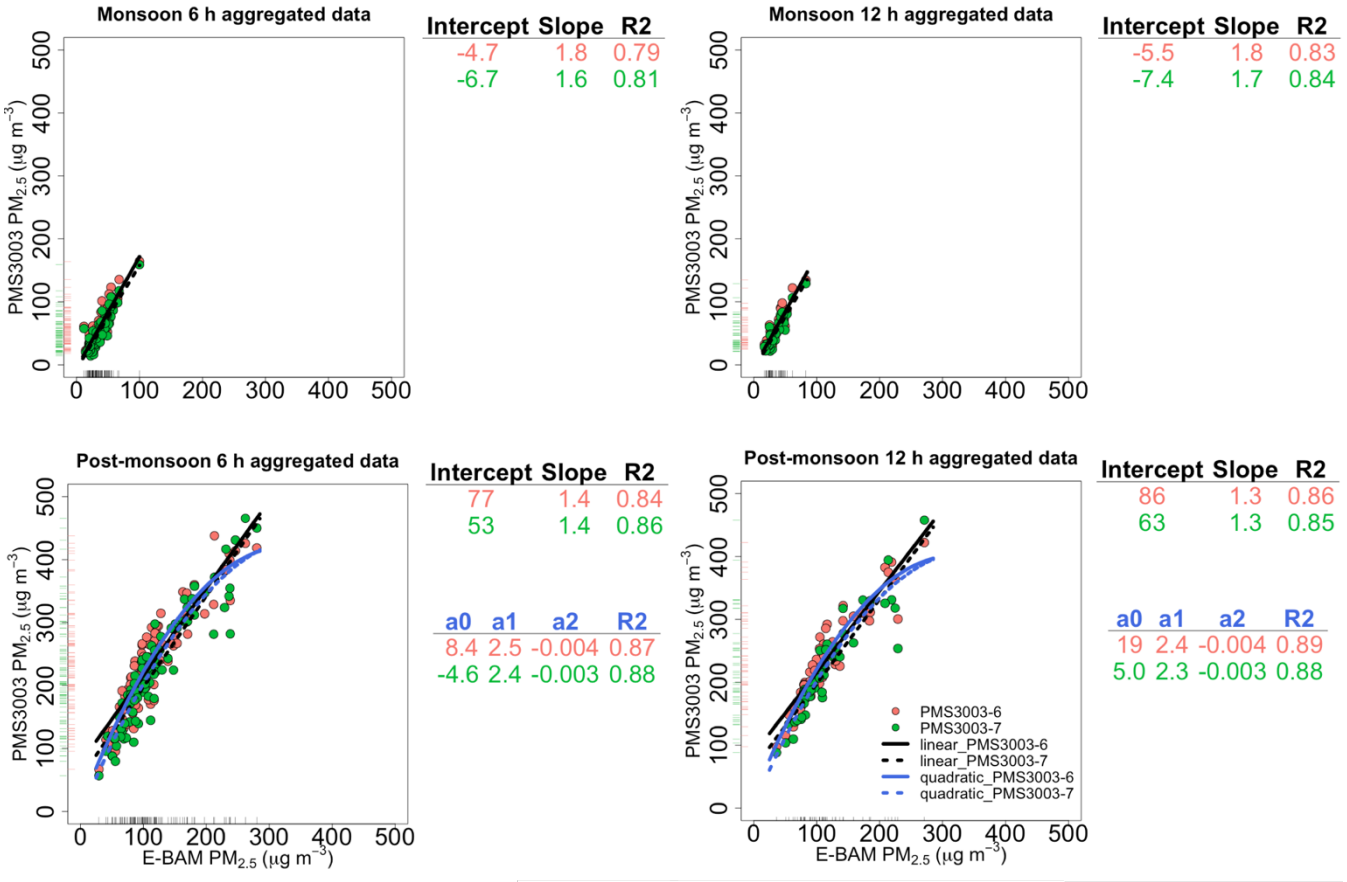

Figure S9: Linear regressions between aggregated $PM_{2.5}$ mass concentrations (µg m^{-3}) of the E-BAM and the two uncalibrated PMS3003s at 6 h and 12 h time intervals during the monsoon season (from June 8, 2017 to June 29, 2017), and the post-monsoon season (from Oct 23, 2017 to Nov 16, 2017) at IIT Kanpur. The fit coefficients for the calibration models are provided. Marginal rugs were added to better visualize the distribution of data on each axis.

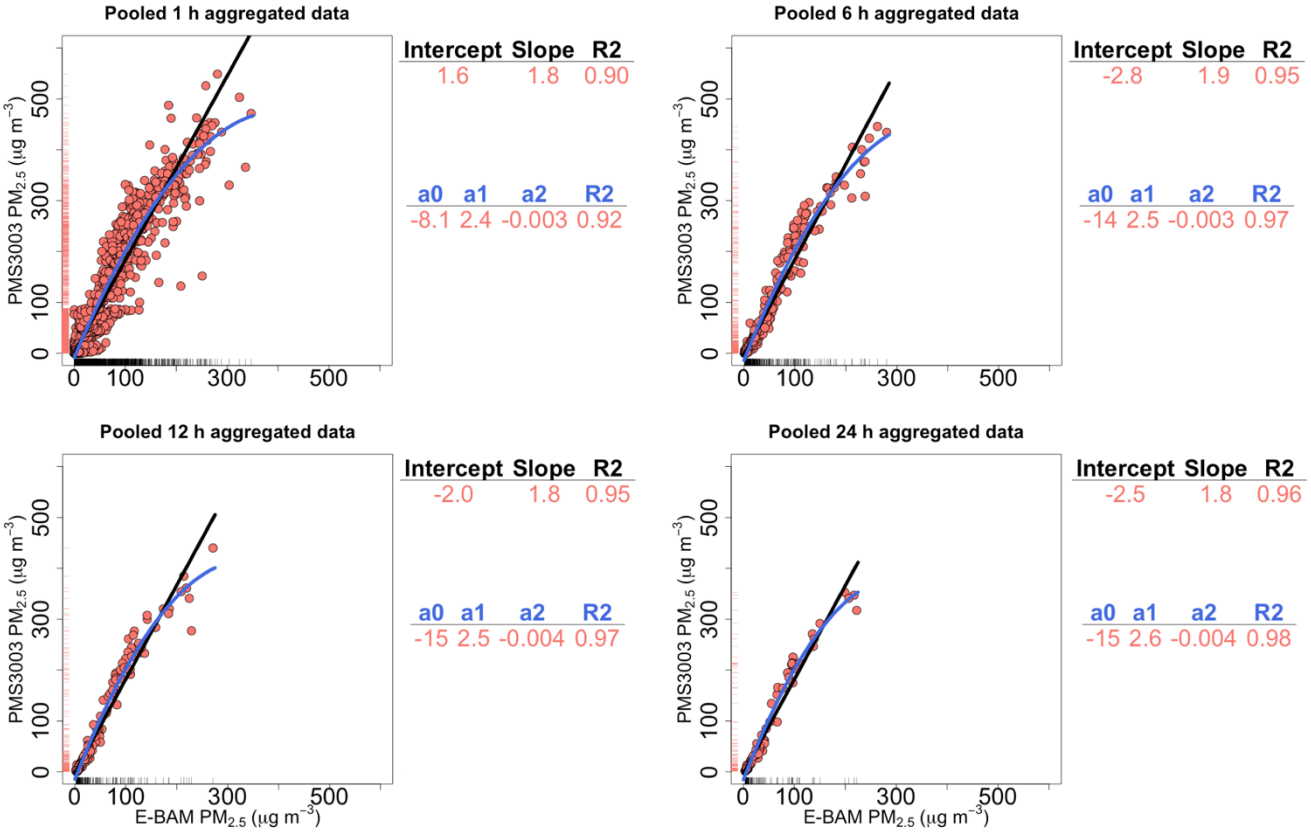

Figure S10: Pairwise correlations between 1 h, 6 h, 12 h, and 24 h aggregated $PM_{2.5}$ mass concentrations (µg m^{-3}) of the E-BAM and the arithmetic means of the uncalibrated PMS3003 sensor package units during each sampling period. The measurements displayed were from the pooled Duke University and IIT Kanpur data sets. Simple linear regression and quadratic lines were superimposed on the pairwise plots. The fit coefficients for the calibration models are provided. Marginal rugs were added to better visualize the distribution of data on each axis.

Table S1: The Akaike's Information Criterion (AIC) was used to determine the significance of the temperature term in the PMS3003 calibration models as a function of averaging timescales for Duke University, US EPA RTP, and IIT Kanpur during monsoon and post-monsoon seasons. The AIC penalizes the complexity of a model. A lower AIC when comparing two models for the same data set indicates a better fitting model. An AIC difference between two models of less than or equal to 2, however, indicates that the two models are roughly the same and therefore the simpler one should be adopted. The finest time resolution for the Duke University and IIT Kanpur data sets was 1 h. The 24 h AIC values are not reported because 24 h observations generally have limited statistical power to determine the significance of temperature in the models. The optimal model at each averaging time interval for each sampling location/season is indicated with shading.

Location/season	Model	1 min	1 h	6 h	12 h	24 h
Duke University	PMS3003 $PM_{2.5}$ conc. $= \beta_0 + \beta_1 \times$ reference $PM_{2.5}$ conc. $+ \beta_2 \times$ temperature	NA	8122	1114	512	NR
	PMS3003 $PM_{2.5}$ conc. $= \beta_0 + \beta_1 \times$ reference $PM_{2.5}$ conc.	NA	8126	1113	510	NR
US EPA RTP	PMS3003 $PM_{2.5}$ conc. $= \beta_0 + \beta_1 \times$ reference $PM_{2.5}$ conc. $+ \beta_2 \times$ temperature	148335	2373	384	266	NR
	PMS3003 $PM_{2.5}$ conc. $= \beta_0 + \beta_1 \times$ reference $PM_{2.5}$ conc.	157757	2563	431	308	NR
IIT Kanpur (monsoon)	PMS3003 $PM_{2.5}$ conc. $= \beta_0 + \beta_1 \times$ reference $PM_{2.5}$ conc. $+ \beta_2 \times$ temperature	NA	3669	577	299	NR
	PMS3003 $PM_{2.5}$ conc. $= \beta_0 + \beta_1 \times$ reference $PM_{2.5}$ conc.	NA	3771	592	301	NR
IIT Kanpur (post-monsoon)	PMS3003 $PM_{2.5}$ conc. $= \beta_0 + \beta_1 \times$ reference $PM_{2.5}$ conc. $+ \beta_2 \times$ temperature	NA	5382	866	435	NR
	PMS3003 $PM_{2.5}$ conc. $= \beta_0 + \beta_1 \times$ reference $PM_{2.5}$ conc.	NA	5710	932	462	NR

NA = not available. NR = not reported.

Table S2: Summary of AIC and RMSE (goodness of fit and accuracy estimates) for the two E-BAM calibrated PMS3003 $PM_{2.5}$ responses during the post-monsoon season at IIT Kanpur, using the simple linear and quadratic calibration methods as a function of time averaging intervals. The results are displayed in mean (range) format. Note the mean statistics were obtained by fitting the models to the PMS3003 $PM_{2.5}$ measurements averaged across the two sensor package units at each point in time. The model that had the best goodness of fit and accuracy estimates at each averaging time interval is indicated with shading.

Timescales	1 h		6 h		12 h		24 h	
Method	Linear	Quadratic	Linear	Quadratic	Linear	Quadratic	Linear	Quadratic[1]
AIC	5731 (5731–5778)	5670 (5670–5720)	932 (932–949)	916 (916–933)	462 (462–474)	454 (454–469)	214 (214–229)	210 (210–225)
RMSE	44 (44–46)	42 (42–44)	30 (30–33)	27 (27–30)	25 (25–29)	23 (23–27)	16 (16–21)	14 (14–19)

[1]The quadratic term (a_2) in the quadratic fit (Eq. (7)) for the PMS3003-6 was not significantly different from 0 (p>0.1).

Table S3: Summary of AIC and RMSE (goodness of fit and accuracy estimates) for the E-BAM calibrated PMS3003 $PM_{2.5}$ results of the pooled Duke University and IIT Kanpur data sets, using the simple linear and quadratic calibration methods as a function of time averaging intervals. Note the values are statistics for the averaged sensor models, which were obtained by fitting the models to the means of PMS3003 $PM_{2.5}$ measurements averaged across all sensor package units during each sampling period. The model that had the best goodness of fit and accuracy estimates at each averaging time interval is indicated with shading.

Timescales	1 h		6 h		12 h		24 h	
Method	Linear	Quadratic	Linear	Quadratic	Linear	Quadratic	Linear	Quadratic
AIC	21005	20638	3376	3225	1697	1590	836	764
RMSE	33	30	23	18	22	16	19	13

[*]All the models' coefficients were statistically significant (p<0.1).